Tamap Journal of Physical Science
http://www.tamap.org/

TJOPS-1812-03
Volume 2018, Article ID 3
Research Article

The Absence of X-ray Luminous Sources in the Galaxy Cluster: AS0296

Hakan SERT[1, 2], Turgay CAGLAR[*3, 2], and H. İlker KAYA[2]

[1] *von Karman Institute for Fluid Dynamics, Chaussée de Waterloo, 72, B-1640 Rhode-St-Genèse, Belgium*
[2] *Physics Department,* Faculty of Science and Art, *Yıldız Technical University,* Istanbul, 34220, Turkey
[3] *Astronomy Department, Leiden Observatory, Leiden University, Leiden, 2380RA, The Netherlands*

Received: 03.12.2018 • **Accepted**: 13.12.2018 • **Published Online:** 15.12.2018

Abstract: In this work, we performed X-ray data analysis to understand possible interactions between inter-cluster medium and member galaxies within Abell S0296 cluster environment. X-ray point-like sources are detected using source detection algorithms. We performed log N - log S in the energy range of 2-10 keV to measure X-ray source number density. The mean intra-cluster medium temperature, abundance, gas density, pressure and X-ray luminosity are found $kT = 2.26 \pm 0.15$ keV, $Z = 0.18 \pm 0.03$ solar, $\rho = 2.52 \pm 0.23 \times 10^{-3}$ cm^{-3}, $P = 5.70 \pm 0.64 \times 10^{-3}$ keV cm^{-3} and $L_X = 1.23 \pm 0.1 \times 10^{43}$ erg s^{-1}, respectively. We find a slightly higher X-ray source over density for Abell S0296 relative to non-clustered fields. Our result reveals that X-ray sources are fainter than expected. Due to lack of high luminous X-ray sources within Abell S0296's cluster potential well, we find evidence that X-ray sources are quenched due to the influence of high cluster mass. We conclude that the main X-ray emissions from point-like sources are produced by X-ray binaries and/or low-luminous active galactic nuclei.

Keywords: galaxies: active – galaxies: clusters: general – X-rays: galaxies: clusters: intracluster medium – galaxies: clusters: Abell S0296

1. INTRODUCTION

Clusters of galaxies are the largest cosmic laboratories that allow us to study the evolution of the universe in detail. Detailed investigations of clusters of galaxies revealed many interesting phenomena of the universe. With an advent in space technology, it has been possible to study the evolution of galaxies and galaxy clusters. Interestingly, detailed X-ray investigations reported an existence of hot inter-cluster medium (ICM) surrounds galaxy clusters vicinities. Unfortunately, the influences of the galaxy cluster environments on the galaxy evolution have not still fully understood. Further investigations are still required to understand the evolution of galaxies within the cluster vicinity.

X-ray source density comparisons between galaxy clusters and non-clustered fields have resulted in an over density phenomena in a favour of galaxy clusters (e.g. [1], [2], [3], [4], [5], [6], [7]). Even so the over density phenomenon is intrinsic for galaxy clusters; it is not certain whether X-ray sources are suppressed or triggered in the cluster environments. Whereas several over density investigations demonstrated suppressions of X-ray sources in the cluster environments [5], [6], [8], [9], the number of the results in favour of triggering of X-ray sources in the galaxy clusters cannot be ignored [10], [11], [12], [13], [14]. Caglar & Hudaverdi (2017) attempted to answer suppression triggering for nearby galaxy clusters. They found evidence for suppression of X-ray sources in the central parts of galaxy clusters, whereas X-ray sources are triggered through the outskirts of the galaxy clusters. In the literature, the very bright X-ray sources are generally used to understand triggering/suppression phenomena, namely Active galactic nuclei (AGN). However, the number of AGNs is rare in the galaxy clusters [7].

* Correspondence: caglar@strw.leidenuniv.nl

The main astrophysical X-ray emission mechanisms are diffuse hot gas, X-ray Binaries (XRBs) and accreting supermassive black holes (SMBHs); therefore, studying dynamical events are key to understand galaxy evolution. In case of absence of AGNs, the off-nuclear sources produce X-ray emission for the quiescent galaxies (e.g. [15], [16], [17]).

In this study, we aim to study the interaction between Abell S0296 and its member galaxies (hereby AS0296). We also intend to measure the X-ray density of AS0296. Our paper is organised as follows: Section 2 reviews observation, data reduction and analysis process. Section 3 describes our measurement method for X-ray analysis. In section 4, we discuss our results due to suppression phenomena, and we present our conclusions. We adopt WMAP standard cosmological parameters $H_0 = 70$ km s^{-1} Mpc^{-1}, $\Omega_M = 0.3$ and $\Omega_\Lambda = 0.7$ in a flat universe.

2. OBSERVATION, DATA REDUCTION AND ANALYSIS

We used archival data of the *XMM-Newton*, which were gathered from the *XMM-Newton* Science Archive (XSA). The observation of AS0296 (OBS ID 0555220301) was performed with a thin filter on 26/02/2008 in full frame mode for MOS and extended full frame mode for pn. The *XMM-Newton* data were processed by using *heasoft 6.25* and *XMMSAS 17.0.0*, and data reduction is explained by Caglar & Hudaverdi (2017) in detail.

2.1 Spatial and Spectral Analysis

SAS source detection algorithms are used to obtain point-like X-ray sources. The SAS task*edetect_chain-3.14.1* was performed using the energy range of 0.2-12.0 keV adopting likelihood values above 10 (about 4 σ) and inside an off-axis angle of 14.5 arcmin. The X-ray source list was combined with SAS task *srcmatch-3.18.1* for MOS and pn cameras. The spectral files are produced by using SAS tasks: *evselect-3.62*, *rmfgen-2.2.1* and *arfgen-1.92.0*. Background spectra were extracted from an annulus surrounding the circular source region. Spectral file areas are calibrated performing *backscale-1.4.2*. Spectral fittings were performed with XSPEC-12.10.1 [18] using redshift dependent photoelectric absorption model ZTBABS and power law within an energy range of 0.3 - 10.0 keV for point-like X-ray sources, and bad data were subtracted from spectra. In addition, thermal plasma model APEC was modelled adopting the abundance table by Lodders (2003) [19].

2.2 Sensitivity of the Survey

The sky coverage represents the survey area of the observed source and decreases with flux due to instrumental effects. The sensitivity of our cameras is estimated using SAS task *esensmap-3.12.1*. The energy conversion factor (ECF) was calculated with XSPEC model (tbabs×power) with a fixed photon index of 1.7 and a fixed total galactic hydrogen column density value. The resulting sky coverage of cameras was used to calibrate the number of X-ray sources that can be detected with the sensitivity of our cameras.

3. METHOD

3.1 Log N – Log S

The number of sources per unit sky area with the flux higher than S, N (> S), can be defined as:

$$N(>S) = \sum_{i=1}^{n} \frac{1}{\Omega_i} \; deg^{-2}$$

where n is the number of detected sources, Ω_i is sky coverage for the flux of the ith source. **Fig. 1** shows log N-log S for our samples and their comparison with Hubble Deep Field North hole result, which was calculated by Caglar & Hudaverdi (2017). Due to low cosmic variance (15%) within 2-10 keV energy range (e.g., [20], [21]); hence, we concentrated on 2-10 keV flux values for our log N - log S measurements.

3.2 Physical ICM Parameters

We performed a spectral analysis to obtain average physical parameters for ICM. The spectral files are generated within 6.5 arcmin radii. The X-ray background was subtracted from spectra using background spectra, which is generated from an annular region of 12 – 13 arcmin. We fit spectra with free kT, abundance and normalisation and a

fixed hydrogen column density and cluster redshift. The average gas densities are obtained from the following equation

$$Norm = \frac{10^{-14}}{4\pi(D_A(1+z))^2} \int n_e\, n_H dV$$

where DA is the angular diameter distance, n_e (electron density) ~ 1.2 n_H (hydrogen density) for a fully-ionised cosmic plasma. Finally, the specific pressure for AS0296 is obtained adopting $P = kT\, n_e$ [22], where kT is plasma temperature. The resulting ICM parameters are presented in Table 1.

4. DISCUSSION and CONCLUSION

We performed *XMM-Newton* data analysis for AS0296. A total number of 72 sources are detected within 14.5 arcmin (see **Fig. 1**). Only 29 X-ray sources are found to be higher than limiting flux 1×10^{-14} erg cm^{-2} s^{-1}. Therefore, log N - log S was performed for this sources at limiting flux value of 1×10^{-14} erg cm^{-2} s^{-1}. We compared log N - log S results for AS0296 and Hubble Deep Field North [7]. The comparison clearly demonstrates that the X-ray source density of AS0296 is slightly higher relative to Hubble Deep Field North (see **Fig. 1**). However, this difference is only found with an offset of 0.2 dex. Overdensity investigations of galaxy clusters demonstrate that the number of X-ray sources is relatively higher in the majority of galaxy clusters than non-clustered fields. Firstly, Cappi et al. (2001) found a 3.5 σ studying two high-redshift galaxy clusters. Other systematic investigations also demonstrated increased source density in high-redshift galaxy cluster environments with an excess > 2 σ (e.g., [23]). In the meantime, low-redshift investigations revealed that the excess in galaxy clusters are also intrinsic for nearby universe [3,7]. In the nearby universe, this excess seems to be due to low luminosity AGN associated with the galaxy cluster, and high luminous AGNs are rare in galaxy cluster environments. Caglar & Hudaverdi (2017) concluded that point-like X-ray sources are suppressed by ICM pressures that force member galaxies to lose their significant amount of fuel. To consider ICM related effects, we fit ICM spectra with a single thermal model. The resulting ICM temperature and abundance are found to be $kT = 2.26 \pm 0.15$ keV, $Z = 0.18 \pm 0.03$ solar. In addition, we estimated mean gas density $\rho = 2.52 \pm 0.23 \times 10^{-3}\ cm^{-3}$ and average pressure $P = 5.70 \pm 0.64 \times 10^{-3}$ keV cm^{-3}. The X-ray luminosity of ICM is also found to be relatively faint $L_X = 1.23 \pm 0.1 \times 10^{43}\ erg\ s^{-1}$. These results indicate that AS0296 hosts a metal-poor, low-density, cold and faint ICM. In **Table 1**, we present the spectral analysis results for the ICM.

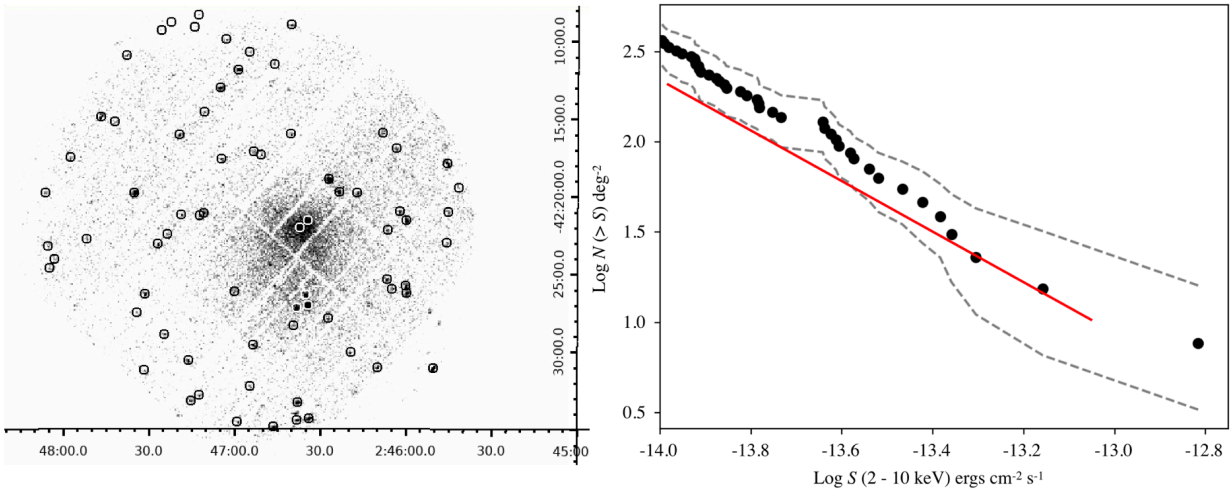

Figure 1: ***Left:*** XMM-Newton mosaic image demonstrating 72 point-like X-ray sources within the field of view. ***Right:*** log N – log S estimated in the energy range of 2-10 keV. The grey dashed lines represent 1σ statistical error. The red solid line is the expected X-Ray source density from the Hubble Deep Field North, which is provided by Caglar & Hudaverdi (2017).

A recent study reported an anti-correlation between X-ray source fraction and cluster mass [24]. The cluster's total and gas mass of AS0296 is reported as M_{total} (< r_{500}) = $1.40 \pm 0.21 \times 10^{14}$ M⊙ and M_{gas} (< r_{500}) $5.47 \pm 0.92 \times 10^{12}$ M⊙ by Sanderson et al. (2013), respectively. The lack of high luminous X-ray sources can be explained by the high X-ray mass of AS0296. Since there is no optical redshifts information for any of our X-ray source in the literature, we assumed the cluster's mean redshift into our X- ray luminosity calculations. The central galaxy of AS0296 (XMMU

J024637.1-422201) is found to be a low-luminosity AGN (log $L_X = 41.43\ erg\ s^{-1}$), whereas there is only one X-ray AGN (XMMU J024550.3-423104) within 1.2 Mpc radius of AS0296. This source is located at the outskirt of AS0296, and X-ray properties of this source results in an X-ray luminosity log $L_X = 42.20\ erg\ s^{-1}$ and hardness ratio HR= −0.42±0.11. In conclusion, X-ray sources of AS0296 are suppressed within AS0296's potential well. In addition, some of the X-ray sources are probably buried inside the ICM; therefore, we cannot detect them. The main astrophysical sources responsible for X-ray point-source emissions are X-ray binaries and low-luminosity AGNs. Finally, further optical investigation and offset X-ray observations are required to understand the evolution of galaxies within AS0296.

Table 1: The resulting ICM parameters obtained from the spectral analysis.

Temperature keV	Abundance $M_\odot$	Gas density 10^{-3} cm^{-3}	Pressure 10^{-3} keV cm^{-3}	X-ray Luminosity erg s^{-1}	Reduced χ^2
2.26±0.15	0.18±0.03	2.52±0.23	5.70±0.64	$1.23\pm0.1 \times 10^{43}$	1.02457

Acknowledgements: The Authors would like to thank the anonymous referee, who improved this article significantly.

REFERENCES

[1] Cappi M. et al., 2001, ApJ, 548, 624
[2] D'Elia V. et al., 2004, NUPHS, 132, 54
[3] Hudaverdi M. et al., 2006, PASJ, 58, 931
[4] Gilmour R., Best P., Almaini O., 2009, MNRAS, 392, 1509
[5] Koulouridis E., Plionis M., 2010, APJ, 714, 181
[6] Ehlert S. et al., 2013, MNRAS, 428, 3509
[7] Caglar T. & Hudaverdi M., 2017, MNRAS, 471, 4990
[8] Haines C. P. et al., 2012, ApJ, 754, 97
[9] Koulouridis E. et al., 2014, A&A, 567, 83
[10] Molnar, S. M., Hughes, J. P., Donahue, M., et al. 2002, ApJ, 573, 91
[11] Martini P., Kelson D. D., Kim E., Mulchaey J. S., Athey A. A., 2006, AJ, 644, 116
[12] Ellison S. L., Patton D. R., Mendel J. T., Scudder J. M., 2011, MNRAS, 418, 2043
[13] Melnyk O. et al., 2013, A&A, 557, 81
[14] Haggard D. et al., 2010, ApJ, 723, 1447
[15] Ho L. C. et al., 2001, 549, 51
[16] Ranalli P., Comastri A., Setti G., 2003, A&A, 399, 39
[17] Ranalli P. et al., 2012, A&A, 542, 16
[18] Arnaud K. A., 1996, ASP, 101, 17
[19] Lodders K., 2003, ApJ, 591, 1220
[20] Cappelluti N. et al., 2005, A&A, 430, 39
[21] Dai X., Griffin R. D., Kochanek C. S., Nugent J. M., Bregman J. N., 2015, ApJs, 218, 8
[22] Caglar, T., 2018, MNRAS, 475, 2870
[23] Ruderman, J. T., Ebeling, H., 2005, APJ, 623, 81
[24] Koulouridis, E. et al. 2018, A&A, 620, 20
[25] Sanderson, Alastair J. R. et al, 2013, MNRAS, 429, 3288